Immediate and Delayed High-Energy Electrons due to Echo 7 Accelerator Operation

R J Nemzek and J R Winckler
School of Physics and Astronomy, University of Minnesota

Abstract:
Detectors on the Echo 7 sounding rocket measured a variety of >1 keV electron pulses resulting from injections of high-energy electron beams. The pulses came from directly-scattered beam electrons, stimulated precipitation of trapped radiation, beam-plasma interactions, and conjugate echoes. The different sources can be distinguished by their delays relative to gun injections- coincident, delayed by 10-100 milliseconds, or delayed by several seconds, respectively.

Introduction:

The Echo 7 sounding rocket, launched 0816:49 UT, 9 Feb. 1988 from Poker Flat, AK, carried a number of detectors designed to measure electrons with energy greater than 1 keV. Most of the instruments were intended to measure 'conjugate echoes'- artificial electron pulses that travel to the southern hemisphere conjugate point and back- but they actually observed a number of immediate and delayed responses to electron gun firing. These included scattered beam particles, ambient electrons accelerated or scattered toward the accelerator payload, particles energized in beam-plasma interactions, and conjugate echoes. Electrons from these different sources can be distinguished from each other by their delay relative to gun firing- the scattered beam electrons and natural particles were observed in coincidence with gun injections, Beam-interaction products were detected 10-100's of milliseconds after injections as they drifted in the payload wake, and the conjugate echoes were measured several seconds after gun pulses as required for their round trip to the southern hemisphere. We will treat each of these processes in turn. The conjugate echo discussion will emphasize payload charging and beam losses rather than the natural magnetospheric properties that can be deduced through the echo technique (see, e.g., Winckler, 1982).

Electron Gun and Instrumentation:

The Echo 7 electron gun operated in two modes: Continuous and Discrete. In Continuous mode, the beam voltage decayed exponentially from 42 kV to 8 kV each millisecond. The gun was a space-charge-limited diode, so the current was proportional to (gun voltage)$^{3/2}$. The current at 42 kV was 225 mA; at 8 kV, 20 mA. All Continuous injections were at 110 degrees pitch angle. Continuous injections were coded in unique groups of 50, 100, and 150 millisecond pulses, to aid in identifying conjugate echo bounce times. Discrete injections

were quasi-DC pulses at 36 keV, 180 mA or 10 keV, 27 mA. 36 keV pulses were 100 or 150 milliseconds long, and were designated by pitch angle as Down (45 degrees), Out (110 degrees) or Up (175 degrees). The 10 keV injections were .95 seconds long, at a pitch angle that was slowly modulated around 90 degrees. Winckler et al. (1989) gave a more complete description of the Echo 7 electron gun.

As explained in Winckler et al. (1989), Echo 7 consisted of a MAIN or accelerator payload and three free-flying subpayloads- NOSE, EPP and PDP. The data presented here will be from a combination of Geiger tubes, scintillation counters, and electron spectrometers flown on the MAIN, PDP, and EPP. A brief description of the instruments follows:

1. Geiger tubes: The Echo 7 Geiger tube experiment was provided by the Air Force Geophysics Lab. Two sets of 4 tubes were flown on the MAIN, one set looking down the magnetic field, the other perpendicular to it. Each set had mica windows with thicknesses resulting in low-energy electron cutoffs at 30, 38, 50, and 75 keV, where the cutoff is defined as half-maximum detection efficiency. The response function for the windows was fairly broad, as shown in Figure 1. The AFGL calibration apparatus only extended to 40 keV, so the upper part of the 50 keV edge and all of the 75 keV edge have been constructed assuming that all the windows had dE/Eo = 25%, where Eo is the half-max energy. This was true for all the measured curves. The widths of the thresholds and the overlap between them complicate analysis somewhat. Each tube was collimated to 45 degrees half-angle and had a geometry factor of .78 cm^2sr. All the tubes accumulated counts with a sample time of 25.6 milliseconds, except the down-looking 30 keV tube, which was read out every 3.2 milliseconds. A roughly 50 microsecond deadtime after each count imposed an upper limit of about 20 kHz count rate. Count rates above about 300 cts/sample seriously underestimated the actual incident flux.

2. The Echo 7 scintillators were very similar to those flown on previous Echo flights. 4500 Å of aluminum on the scintillation crystal's front surface established an approximately 1 keV lower energy threshold. The phototube output was read as a current and sent through a 5-decade log amplifier. The scintillators were collimated to 13 degrees half-angle and had a .13 cm^2sr geometry factor. The absolute energy flux calibration of the scintillators has not been completed. Four scintillators were flown on the PDP and EPP, one every 90 degrees in azimuth. The MAIN held two scintillators, one looking up at electrons with 0 degrees pitch; the other looking parallel to the injected beam, detecting electrons at 70 degrees pitch angle. Scintillators on the PDP and EPP were sampled at 625 Hz, while the up-looking MAIN scintillator was read at 2500 Hz and the out-looking tube at 5000 Hz.

3. TED's: The Toroidal Electron Detectors (TED's) were curved-plate electron spectrometers with geometry factors of about $5x10^{-3}$ cm^2 sr keV. They measured electron energies to 7.5% resolution, from 2 keV to 40 keV. The detectors accumulated counts during 32, 1.6 millisecond steps, for a complete sweep time of 51.2 milliseconds. EPP and PDP each had two TED's, 180 degrees apart, perpendicular to the subpayload spin axis (EPP) or 80 degrees from the spin axis (PDP). Only EPP TED 2 and PDP TED 2 functioned properly.

Measurements:

The electron measurements made by the Echo 7 high-energy electron detectors can be separated into several categories: the natural trapped radiation background; "immediate responses," electrons observed by MAIN payload detectors in coincidence with accelerator operation; "prompt responses," apparent products of a beam interaction observed in the payload wake after a short time delay; and "conjugate echoes," electrons which returned to the payload after several seconds of travel through the magnetosphere.

Background:

Figure 2 shows the high-energy background measured by the Geiger tubes perpendicular to B during gun off times. The down-looking detectors measured <<1 ct/sample. The various Geiger tube channels showed similar temporal features. Counts in the >30 and >38 keV channels were approximately equal, while the >50 kev count rate was slightly lower and the >75 keV rate was only about .3x the rates in the lower-energy channels. This implies a spectrum with electrons primarily above 40 keV, trailing off above 50 keV. Main payload telemetry failed after 325 seconds flight time.

Immediate Responses:

During gun operation, all of the Geiger tubes showed an increased electron flux. Since most injections were at 36 kV or below 42 kV, the > 75 keV channel should not have been greatly affected by scattered gun electrons, although lower channels were probably severely contaminated by this source. Count rates began to increase simultaneously with injections, and built up to a maximum over a roughly 10 millisecond period. At the end of gun pulses, count rates declined to zero in the same length of time. Figure 3 shows the response of the out and down detectors to Continuous injections. Figure 4 is the same for Discrete Out injections, which produced the most intense response in the Geiger tubes. All channels in Figure 4 except the >75 keV curve were saturated. At 250 seconds the flux became so intense that the tubes went into a constant discharge and virtually stopped counting. The count rate at this time was likely >1 MHz. Down and Up injection responses were several times less intense than those from the Out pulses. 10 keV injections produced a slight but definite increase in all Geiger tube channels. This shows that at least some of the Geiger tube signals were

likely produced by electrons far above the beam energy. We are assuming that the Geiger tube responses all were due to electrons. If x-rays from beam electrons were present in sufficient numbers, the analysis of the Geiger tube data could be quite different. Even low energy x-rays could penetrate the high energy windows of the tubes.

Comparing Figures 3 and 4 to Figure 2, it is clear that several features are the same in each- e.g., the peaks at 260 and 310 seconds. This indicates that some of the high-energy electrons counted by the Geiger tubes were probably precipitated natural particles. The electron beam opened the loss cone above the rocket, allowing the formerly trapped radiation to propagate downward. This result would take a substantial change in pitch angle- electrons at 90 degrees pitch above the rocket would need their pitch angles reduced by 45 degrees in order to mirror and return within the solid angle of the down-looking detectors. A pitch angle of 70 degrees, however, would allow electrons to intercept the 100-km atmosphere; thus most of the upward-travelling electrons are likely backscattered from the atmosphere. Count rates in the 75 keV out- and down-looking channels were about equal, so the flux reaching the rocket must have been nearly isotropic. The count rate increases near 190 seconds and 310 seconds were relatively large compared to the corresponding change in the background rate. This may be the result of enhanced precipitation and beam scattering at lower altitudes; apogee was at 281 seconds.

The Trigger (Bering et al., 1982), Araks (bering et al., 1982) and G-60-S (Managadze et al., 1988) active experiments all measured precipitation of trapped electrons through electron beam perturbation. The Trigger and Araks precipitation, though, was delayed by several seconds with respect to the perturbation, pointing to an interaction occurring out in the magnetosphere. The Echo 7 precipitation and that during G-60-S was coincident with electron beam operation. The G-60-S precipitation was inversely related to payload potential. A similar dependence of precipitation on payload potential may be responsible for the 'altitude effect' resulting in the large flux increases near 190 and 310 seconds flight time as mentioned above.

At present we do not have a complete understanding of the physical process culminating in the precipitation. As discussed above, the precipitation began immediately upon electron injection but required some time both to build up to full intensity and to die away, so the bulk of the scattering probably occurred well above the payload, up to 100 km away. The ratios of the count rates in the >75 keV channels between various injection modes show that the precipitation was greater for high energy-high current gun pulses. This may not be a simple relationship, though. The precipitation during Discrete, 110 degree injections was up to several

hundred times that during Continuous, 110 degree injections, even though the Discrete gun current was only 2.3x the average Continuous injection current. Also, if the payload potential-precipitation connection found by G-60-S operated during Echo 7, the precipitation would have been favored during Continuous injections, which had payload potentials several times lower than Discrete injections (Winckler et al., 1989).

W.J. Burke (personal communication, 1988) has suggested that the loss cone might be opened, allowing precipitation, by the removal of a downward parallel electric field above the payload. The parallel field would be that associated with a local field-aligned current. The beam electrons plus the ambient electrons heated by the plasma might constitute enough downward current to eliminate the need for a parallel electric field to supply the Region 2 field-aligned current. If the beam-produced current was sufficient, an upward parallel electric field might even develop. The loss or reversal of the pre-existing field would then lower the mirror points of the trapped radiation to the payload altitude. A 20° change in pitch angle for a 50 keV electron would require a 5 kV field-aligned potential. We do not have any evidence for the existence of field-aligned currents or large parallel electric fields above the Echo 7 payload.

The MAIN payload scintillators also showed a response coincident with gun pulses. This was primarily composed of gun-energy and lower electrons. The scintillator signal oscillated with the gun drive frequency, 1 kHz. At gun turn on there was often a transient amplitude increase in the oscillations up to 100x the steady-state amplitude. This was also shown by the Geiger tubes (Figure 5). The transient had a harder spectrum than the precipitating radiation. So it appears that the payload initially charged to a significant fraction of the beam voltage and settled back to a steady-state value after about 15 milliseconds. The MAIN payload tether measured an average 2 kV potential during Continuous injections at apogee (Winckler et al., 1989).

Immediately following beam turn-off, the MAIN scintillators measured a short burst of electrons. As altitude increased, the maximum of the burst came progressively later than beam turn-off, being about 10 milliseconds after near apogee (Figure 6). The effect was present even in injections that were disturbed by ACS gas injections, which wiped out practically all other high-energy electrons. Some suprathermal electrons in the hot plasma region could be energetic enough to be counted by the scintillators, but the burst was only at 0 degrees pitch angle. Such a field-aligned pulse of electrons could occur if there was a parallel potential above the payload after beam turn-off. MAIMIK measured a positive payload potential occurring ≈10 milliseconds after a gun pulse (Maehlum et al., 1988), but

this was only about 10 V; the Echo 7 scintillator data require a potential of at least 1 kV to accelerate the electrons.

Prompt Responses

Detectors on the EPP, positioned to the west of the accelerator payload, measured electron pulses delayed by 10-180 milliseconds with respect to gun injections. The location of the EPP means that it was in the general direction of the payload plasma wake, as determined by the combination of ExB drift and the negative of the payload velocity vector. We have dubbed the delayed pulses "prompt responses," in keeping with terminology used for similar events observed during the SCEX I flight (Wilhelm et al., 1985). The best prompt response measurements came from EPP TED2, although the EPP scintillators also detected them. The prompt responses were composed of electrons covering the full 2-40 keV range of TED2, with a differential spectrum proportional to $E^{-3/2}$ The raw data, Figure 7, demonstrates that the responses were most intense for discrete injections near 90 degrees, and that the delay between gun pulse and prompt response increased with flight time- i.e., with increasing distance between the MAIN and EPP. The delay increased almost linearly with distance (Figure 8); the slope of the line in Figure 8 corresponds to a speed of about 1500 m/sec, comparable to the plasma drift velocity in the payload frame. The delays in Figure 8 were determined by measuring the time from the start of a gun pulse to the beginning of the response, regardless of what energy the analyzer was reading at that time. Obviously, there was little dispersion in arrival times between high and low energies.

Our model for creation of the prompt response events is this: when the gun fired, a beam interaction created a flux tube filled with electrons of a wide range of energies, even above the beam energy. This flux tube drifted back into the payload wake region. After some time, it intercepted the EPP, causing the measured prompt response. As the EPP moved away, the drift time increased. Since electrons of all energies drifted at the same speed- gradient-curvature drift was negligible at these low altitudes- there was no dispersion in arrival times. High and low energies would, however, have had to start from different altitudes. The longest measured delays were 180 msec (for 100 and 150 msec injections!). It would be difficult to trap a 40 keV electron near the payload for that amount of time, so the particles must have come from very high altitudes. A 40 keV electron would have to start near 2000 km altitude to be part of a response delayed by 180 msec. The full range of electron energies would be created at these high altitudes, but only the high energies would be able to propagate back down to the payload in time. The delays in Figure 8 go to zero at a perpendicular distance of 60 m; this is the approximate lateral size of the flux tube.

As the 2000 km-tall flux tube moved back into the payload wake, its particle population diminished. Figure 9 shows this exponential decay expressed in the flux of 10 keV electrons. The flux dropped off with a 1/e time of about 50 msec. This lifetime and the size quoted above are comparable to those measured for near-rocket 'halos' on Echo 3 (Arnoldy and Winckler, 1981) and Polar 5 (Maehlum et al., 1980). The halos may be the part of the prompt response flux tube nearest the accelerator payload.

The "Out" prompt responses were usually 50-60 msec longer than gun pulses. The responses existed in any one location for the length of the gun pulse plus the time for the flux tube to drift over the subpayload after gun operation ceased. If we assume a nominal 1500 m/sec plasma drift speed, the extra 50 msec is equivalent to a flux tube 75m across, similar to the size derived from the 0-drift-time intercept. When the response amplitude dropped to near zero- around 260 seconds and after 400 seconds in Figure 9- the responses were only as long as gun pulses. At these times the subpayload must have been just grazing the flux tube edge. So it appears that the EPP was in the plasma wake at gun turn-on, moved out of it by 260 seconds flight time, then moved back into it until the prompt responses died away after 400 seconds.

If the ionospheric convection electric fields were nearly constant, as they appear to have been (K.N. Erickson, personal communication, 1989), the EPP should have crossed the flux tube during a single time interval. The movement of the flux tube across the EPP twice may indicate that large-scale, beam-produced electric fields were affecting the flux tube's motion. This might also explain why the drift speeds for prompt responses from Down and Up injections were significantly lower than Out drift speeds: 1000 m/s and 600 m/s, respectively, vs. 1500 m/sec.

The prompt responses appear to have been a major beam power loss mechanism. If we take the prompt response amplitude closest to the payload and assume that it was constant over a 60 m radius, 2000 km tall cylinder, the integrated flux is equivalent to 1000x the total beam power. This is a serious problem. In our mechanism the prompt response power should have come from the injected beam. This discrepancy might be resolved in two ways: by limiting the height of the interaction region, or by reducing the effectiveness of the interaction with height. The 2000 km height came from the very long delay times combined with high-energy electrons; if some trapping mechanism was functioning, the electrons would not have to come from such high altitudes. Trapping could be accomplished by parallel electric fields, but they would have to be on the order of 5 kV total potential. The calculation above assumed that the prompt response amplitude was constant along the entire flux tube. This was certainly not the case.

The relative prompt response intensities during injections at different pitch angles show that the prompt response interaction was maximized for injections near 90 degrees. As the beam propagated to higher and higher altitudes, its pitch angle would have decreased, so the prompt response mechanism would have become less effective with altitude. If the prompt response intensity decreased with altitude, it would change the interpretation of Figure 9. If the power calculation is correct, then the energy for the prompt responses must have come from a non-beam source- perhaps the trapped radiation or the diffuse auroral flux.

The prompt responses likely were caused by an interaction of the beam with the trapped radiation. This source would not only alleviate the prompt response power dilemma but also would present a natural way of providing electrons with very high energies without having to energize ambient plasma electrons to greater than beam energy. Most of the high-energy electrons in the responses probably were not beam particles since their spectrum had no hint of a peak at beam energy. The spectrum was likely not the true trapped radiation spectrum either, but rather the trapped energy distribution modified by the interaction.

One may ask whether the prompt responses were identical to the stimulated precipitation measured by the MAIN Geiger tubes. They apparently were somewhat different phenomena. The prompt responses had an intensity that continually decayed with distance from the MAIN payload, with none of the structure evident in the Geiger tube data. Still, they do both appear to be expressions of stimulated precipitation. The Geiger tubes may have been responding primarily to electrons with energies far above the TED energy range. The prompt responses should have been energetic enough to be counted by the Geiger tubes. The prompt responses probably contributed to a constant count rate in the Geiger tubes, especially during the discrete injections, when the prompt responses were most intense. The MAIN payload would have been on the southern edge of the prompt response region, and the generally westward plasma drift would drag the region away from the MAIN. Therefore any prompt responses measured on the MAIN would only be as long as gun pulses, not longer as the EPP prompt responses usually were.

Conjugate Echoes

Conjugate echoes occur when an electron beam injected in the ionosphere spirals out into the magnetosphere, mirrors or scatters at the conjugate point, and returns to the injecting payload. Whether an echo pulse returns to the payload position exactly or just to the vicinity depends on a vector cancellation between payload velocity perpendicular to B and bounce-average particle drift (gradient-curvature drift and ExB drift). A complete examination of conjugate echo theory can be found in Winckler (1982).

The detection of conjugate echoes was the main purpose behind all flights in the Echo program. Echoes resulting from artificial electron injection can be used to elucidate several properties of the magnetosphere- field line geometry, ionospheric electric field mapping, and equatorial pitch angle diffusion. In the present context, echo measurements can put limits on payload charging and beam power loss.

All Echo 7 particle instruments designed for electron energies greater than a few keV measured echoes, although the scintillators and Geiger tubes on the MAIN were practically useless for conjugate echo work because of interference from the intense immediate electron fluxes that resulted from gun operation. Most of the echo instrumentation was on the free-flying PDP and EPP, which drifted well outside the region of serious gun disturbances. Fortunately the prompt responses described in the previous section did not greatly interfere with echo measurements.

One of the best sequences of conjugate echoes is shown in Figure 10a. The timing and widths of the scintillator pulses match almost exactly with the sequence of gun pulses shown below them- but the electrons arrived at the scintillators about 2.8 sec after they left the accelerator. This means that the time for a complete bounce to and from the conjugate point was 2.8 seconds. Figure 10b shows the energy measurement for two individual pulses from 10a- they were nearly monoenergetic at about 18 keV. This was expected due to the spectrometer action of the magnetosphere. The gradient-curvature drift is energy dependent, so the initial continuous-energy pulses were spread out into a kilometer-long east-west oriented sheet, high energies to the east and low energies to the west. This effect increased the area over which echoes could be detected, and was the motivation behind the use of Continuous injections. The energy measured at the payload position depended on the values of eastward payload velocity and ExB drift present at the time of injection. The measured echo energy changed during the flight, probably due to changing northward electric fields, and so we were able to construct a bounce time-energy diagram (Figure 11). The solid line in the Figure was calculated by numerically tracing electron trajectories through the Olson-Pfitzer quiet time magnetic field model (Olson and Pfitzer, 1977). This demonstrates both that the Olson-Pfitzer model is a reasonable fit to the real magnetosphere during the Echo 7 flight, and that the echoing particles travelled adiabatically.

Echo energy/bounce measurements should not have been affected greatly by moderate levels of payload charging. The initial beam had a continuous energy spectrum; a payload potential would have shifted the spectrum as a whole. As long as payload charging did not slow the entire beam below the adiabatic echo energy, echoes would still return. If the energy change occurred less than an Earth radius or so from the

payload, it would not have a large effect on the total bounce time. The free flyers were far enough away from the MAIN that charging did not alter the energy of returning echoes.

Payload potentials must have been less than the difference between the maximum beam energy and the echo energy. For the data in Figure 11, this puts an upper limit of 20 kV on payload charging. There are many echoes that could not be shown in Figure 11 because they did not have easily determined bounce times. They probably came from Continuous injections. The highest energy echo found as yet was at 34 keV, giving a payload potential upper limit of 8 kV. The MAIN payload tether measured an average potential of 2 kV during continuous injections (Winckler et al., 1989). The tether indicated payload potentials of >5 kV during 36 kV Discrete injections. Unfortunately, the one echo known to have come from a Discrete injection apparently underwent some non-adiabatic process during its bounce (Nemzek and Winckler, 1989) and so can't be used in a simple analysis of payload charging.

The echoes prove that a fraction of the beam escaped to "infinity," in a steady-state fashion. Fast pulsed emission such as theorized by Winglee and Pritchett (1987) would appear to be identical to continuous emission in the echo measurements. We have estimated the total fraction of beam current returning to the rocket altitude in conjugate echoes. We assumed that an echo occupied an area 2 gyrodiameters on a side. This is justified by Echo 4 measurements, which demonstrated that an echo retains a size on the order of a gyrodiameter (Winckler, 1982). We have also assumed that the echoes were monoenergetic and isotropic over the upper hemisphere; Echo 7 echoes had electrons with pitch angles from >90 degrees down to at least 45 degrees. With these assumptions, the intensities measured by the TED's for the echoes shown in Figure 10 were equivalent to a current 1.3 x 10^{15} electrons/second. This current is integrated across the entire area occupied by the 18-keV echoes. This is about 20% of the average beam current at the echo energy. If there was significant payload charging then the echo current should be compared to the gun current at a higher voltage, corresponding to the energy of the echoing electrons when they left the gun. For 2 kV charging during continuous injections, this gives an echo current equal to 17% of the initial beam current. The lack of optically-observed echoes put an upper limit of 8% on the returning beam current in Discrete injections, which had much more power than the Continuous injections (Winckler et al., 1989). The discrepancy between the fraction of the beam returning for the two types of injections indicates that the Discrete injections underwent an increased interaction that the Continuous beams did not. The prompt response mechanism had this behavior: Discrete beams resulted in much higher fluxes than did Continuous pulses. The amount of beam returning to

the rocket also appears to be dependent on the level of geomagnetic activity (Winckler et al., 1988).

Conclusion:

This paper presents only a fraction of the phenomena measured by the Echo 7 electron detectors. While these data cover diverse topics, there is a common thread linking several explanations: a natural or beam-induced parallel electric field above the payload. Still, we have no direct evidence to confirm the existence of such a field, and the speculation about a parallel electric field in this paper does not even constitute circumstantial evidence. Indeed, if there was an upward field with ≈5 kV total potential above the payload, many of the conjugate echoes would not have escaped the payload region at all. More detailed examination of the echo bounce times and energies will allow us to put an upper limit on the total parallel potential above the payload.

Acknowledgements:
The Winckler group at the University of Minnesota is supported by NASA grant NSG5088. R.J. Nemzek was supported throughout most of the Echo 7 project by NASA grant NGT50009, administered through the NASA Graduate Student Researchers Program. Special thanks goes to K.A. Lynch of the University of New Hampshire, who constructed the Echo 7 Geiger tube experiment while at AFGL.

References:

Arnoldy, R.L., and J.R. Winckler, The hot plasma environment and floating potentials of an electron-beam-emitting rocket in the ionosphere, J. Geophys. Res., 86, 575-584, 1981.

Bering, E., J. Benbrook, J. Roeder, and W. Sheldon, Evidence for beam-stimulated precipitation of high-energy electrons, in Artificial Particle Beams in Space Plasma Studies, B. Grandal, ed., 147-157, Plenum, 1982.

Maehlum, B.N., B. Grandal, T.A. Jacobsen, and J. Troim, Polar 5- An electron accelerator experiment within an aurora. 2. Scattering of an artificially produced electron beam in the atmosphere, Planet. Space Sci., 28, 279-289, 1980.

Maehlum, B.N., J.Troim, N.C. Maynard, W.F. Denig, M. Freidrich, and K.M. Torkar, Studies of the electrical charging of the tethered electron accelerator mother-daughter rocket MAIMIK, Geophys. Res. Lett., 15, 725, 1988.

Managadze, G. G., V.M. Balebanov, A.A. Burchudladze, T.I. Gagua, N.A. Leonov, S.B. Lyachov, A.A. Martinson, A.D. Mayorov, W.K. Riedler, M.F. Friedrich, K.M. Torkar, A.N. Laliashvili, Z. Klos, and Z. Zbyszynski, Potential observations of an electron-beam emitting rocket payload and

other related plasma measurements, Planet. Space Sci., 36, 399-410, 1988.

Nemzek, R.J. and J.R. Winckler, Non-adiabatic conjugate electron echoes due to Echo 7 accelerator operation (abstract), EOS trans., in press, 1989

Olson, W.P. and K.A. Pfitzer, Magnetospheric magnetic field modeling, McDonnel-Douglas Astronautics Co., Annual Science Report, AFOSR Contract F-44620-75-C-0033, 5301 Bolsa Ave., Huntington Beach, CA, 92647, 1977.

Wilhelm, K., W. Bernstein, P.J. Kellogg, and B.A. Whalen, Fast magnetospheric echoes of energetic electron beams, J. Geophys. Res., 90, 491, 1985.

Winckler, J.R., R.J. Nemzek, R.L. Arnoldy, and T.J. Hallinan, ECHO electron beam experiments in the diffuse aurora (abstract), EOS trans., 69, 1368, 1988.

Winckler, J.R., The use of artificial electron beams as probes of the distant magnetosphere, in Artificial Particle Beams in Space Plasma Studies, B. Grandal, ed., 3-34, Plenum, 1982.

Winckler, J.R., P.R. Malcolm, R.L. Arnoldy, W.J. Burke, K.N. Erickson, J. Ernstmeyer, R.C. Franz, T.J. Hallinan, P.J. Kellogg, S.J. Monson, K.A. Lynch, G. Murphy, and R.J. Nemzek, ECHO 7: An electron beam experiment in the magnetosphere, Eos, 70, 657,666-668, 1989

Winglee, R.M., and P.L. Pritchett, Space charge effects during the injection of dense electron beams into space plasmas, J. Geophys. Res., 92, 6114-6126, 1987.

Figure Captions:

Figure 1. Echo 7 Geiger tube thresholds: Relative detection efficiency was measured for low energies (solid curves) and reconstructed for high energies (dashed curves). Energies of Discrete and Continuous accelerator pulses are marked.

Figure 2. Geiger tube background: The Geiger tubes oriented at 90° to B measured trapped radiation >40 keV during gun off times. Measurements are plotted every 5 seconds.

Figure 3. Geiger tube response to continuous injections: During Continuous injections, both 90 degree (top) and 180 (bottom) Geiger tubes measured enhanced count rates. The peak at 260 seconds is also found in Geiger tube background measurements. Data are plotted once every 10 seconds.

Figure 4. Geiger tube response to Out injections: 36 kV, 180 mA discrete injections at 110 degrees produced the largest Geiger tube count rates. Only the >75 keV channels were not saturated. The notch at 250 seconds was caused by extremely high count rates shutting down the Geiger tubes.

Figure 5. Transient particle flux increase at start of gun pulse: Scintillator and Geiger tube responses to injections often started with a sharp increase which died away to a steady-state value after about 15 msec.

Figure 6. Field-aligned electron bursts after injections: At the end of gun pulses, the scintillator looking parallel to B measured a pulse of electrons. As the payload approached apogee, the bursts separated from the injections.

Figure 7. Prompt Responses: EPP TED2 measured a broad spectrum of electrons produced by gun firing. The prompt responses delay increased as the EPP moved away from the MAIN.

Figure 8. Prompt Response delays: The delay between gun pulse and prompt response increased nearly linearly with perpendicular distance between the EPP and MAIN.

Figure 9. Prompt Response decay: The prompt response amplitude for 10 keV electrons decayed exponentially as the EPP moved away from the MAIN. Near 260 seconds and after 400 seconds the amplitude dropped to 0.

Figure 10 a. Scintillator echoes: Pulses measured by the PDP scintillators matched gun pulses emitted 2.8 seconds earlier.
b. PDP TED2 measurements of individual scintillator echo pulses show that the echoes were monoenergetic at 18 keV.

Figure 11. Energy-bounce time plot: The various echo energy-bounce time pairs match well with calculations made by tracing field lines in the Olson-Pfitzer field model.

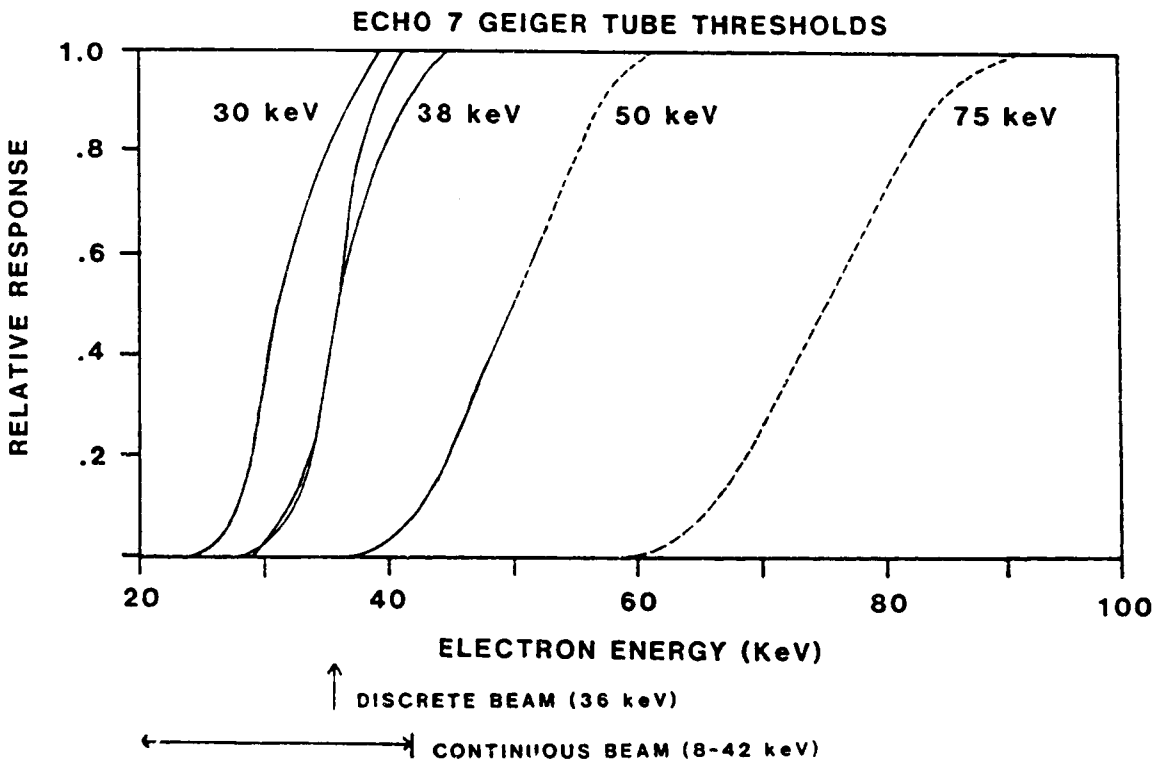
ECHO 7 GEIGER TUBE THRESHOLDS
RELATIVE RESPONSE
1.0
.8
.6
.4
.2
30 keV
38 keV
50 keV
75 keV
20
40
60
80
100
ELECTRON ENERGY (KeV)
DISCRETE BEAM (36 keV)
CONTINUOUS BEAM (8-42 keV)

FIGURE 1

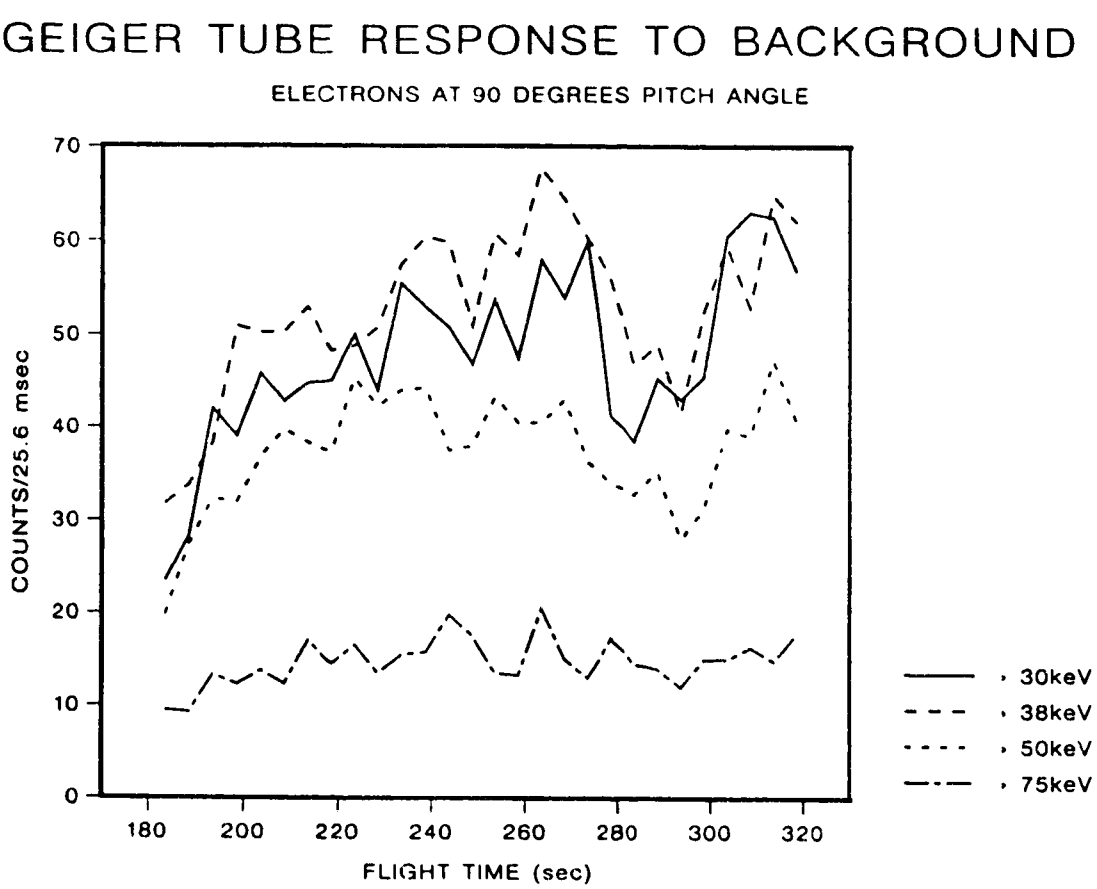
GEIGER TUBE RESPONSE TO BACKGROUND
ELECTRONS AT 90 DEGREES PITCH ANGLE
COUNTS/25.6 msec
0
10
20
30
40
50
60
70
180
200
220
240
260
280
300
320
FLIGHT TIME (sec)
30keV
38keV
50keV
75keV

FIGURE 2

GEIGER TUBE RESPONSE TO CONTINUOUS INJECTIONS

ELECTRONS AT 90 DEGREES PITCH ANGLE

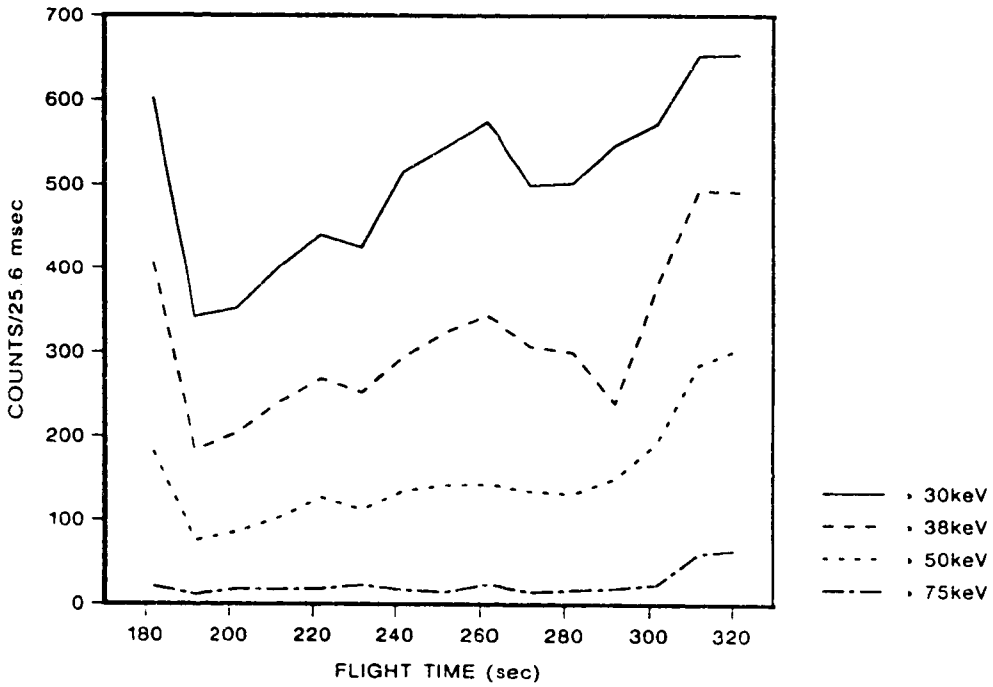

GEIGER TUBE RESPONSE TO CONTINUOUS INJECTIONS

ELECTRONS AT 180 DEGREES PITCH ANGLE

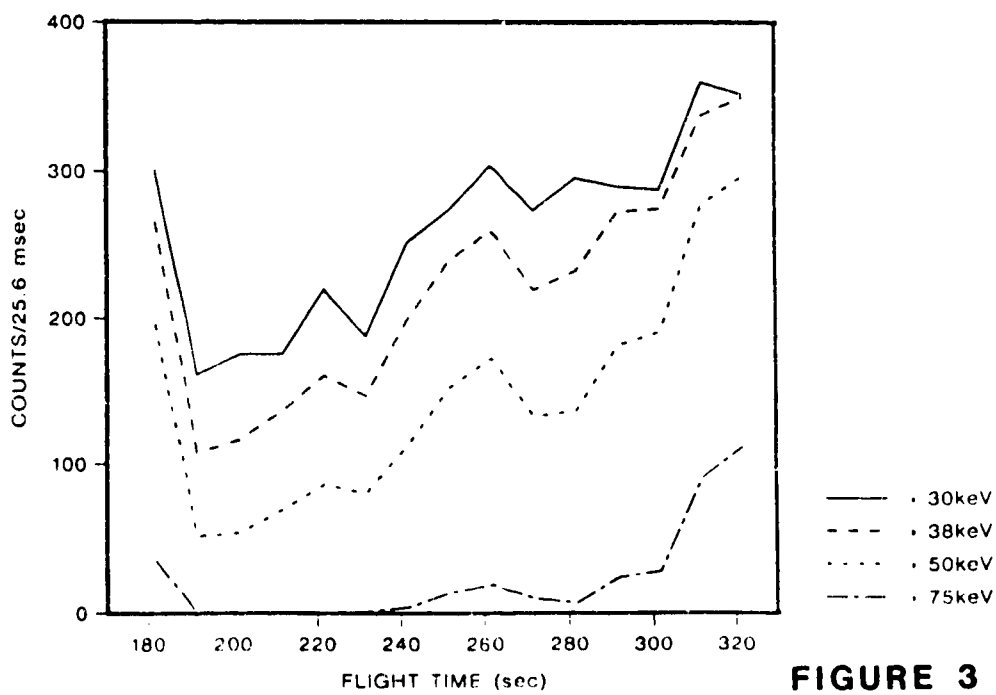

FIGURE 3

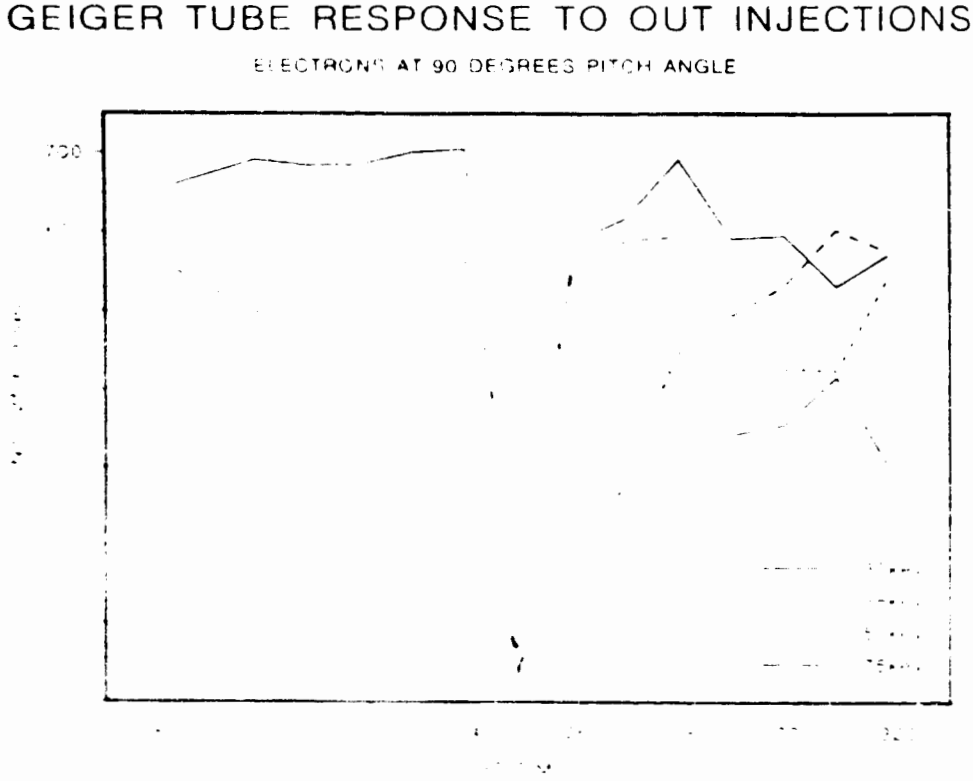
GEIGER TUBE RESPONSE TO OUT INJECTIONS
ELECTRONS AT 90 DEGREES PITCH ANGLE

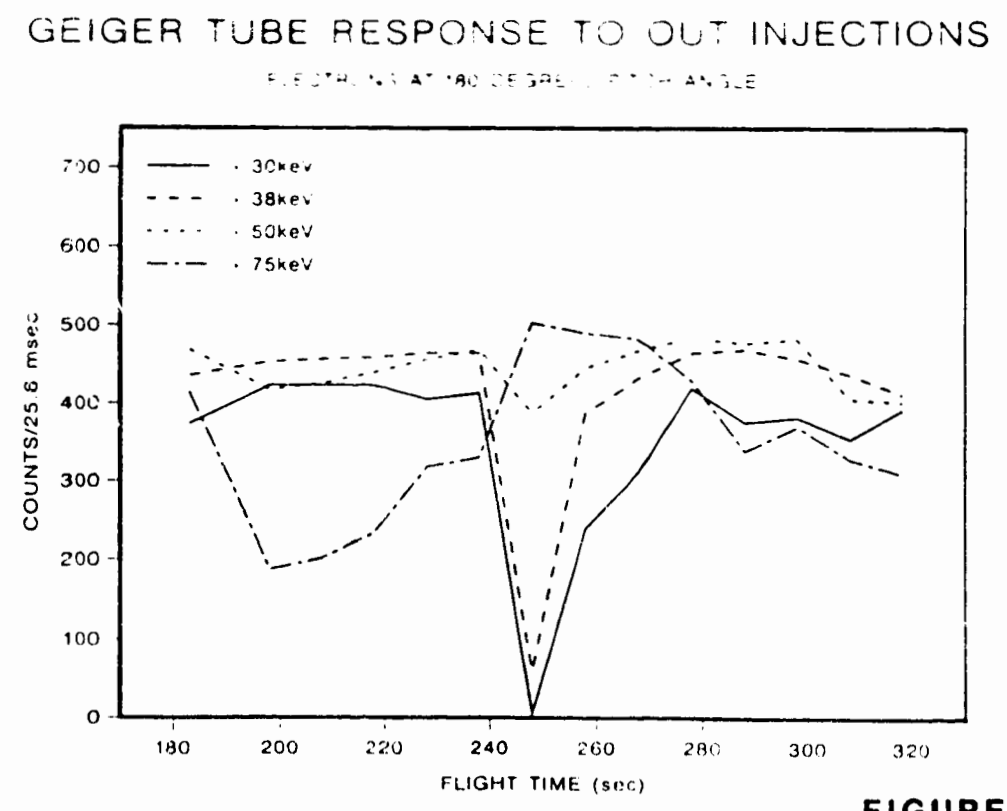
GEIGER TUBE RESPONSE TO OUT INJECTIONS
30kev
38kev
50keV
75keV
COUNTS/25.6 msec
0
100
200
300
400
500
600
700
180
200
220
240
260
280
300
320
FLIGHT TIME (sec)

FIGURE 4

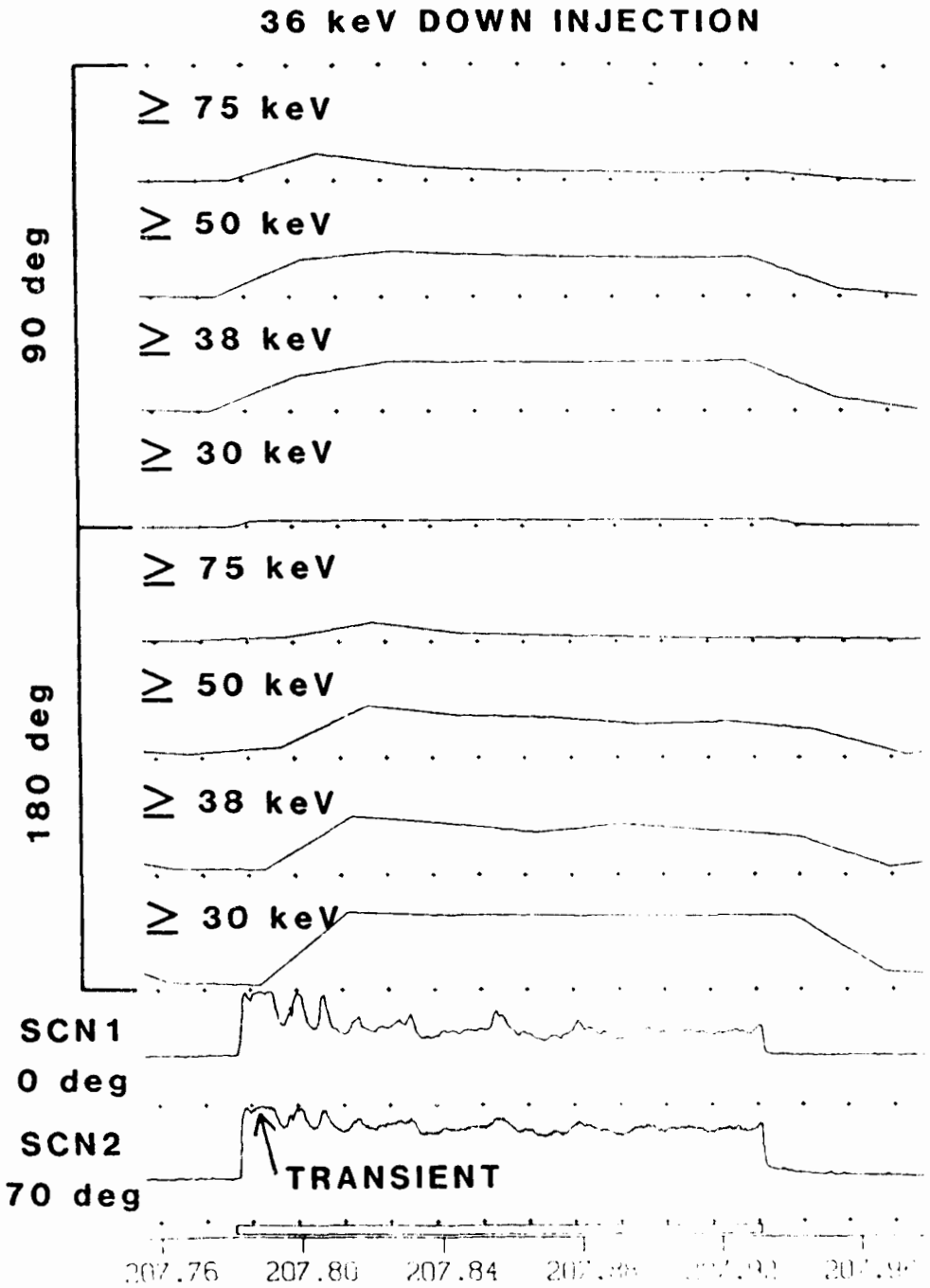
36 keV DOWN INJECTION
90 deg
≥ 75 keV
≥ 50 keV
≥ 38 keV
≥ 30 keV
180 deg
≥ 75 keV
≥ 50 keV
≥ 38 keV
≥ 30 keV
SCN1
0 deg
SCN2
70 deg
TRANSIENT
207.76
207.80
207.84

FIGURE 5

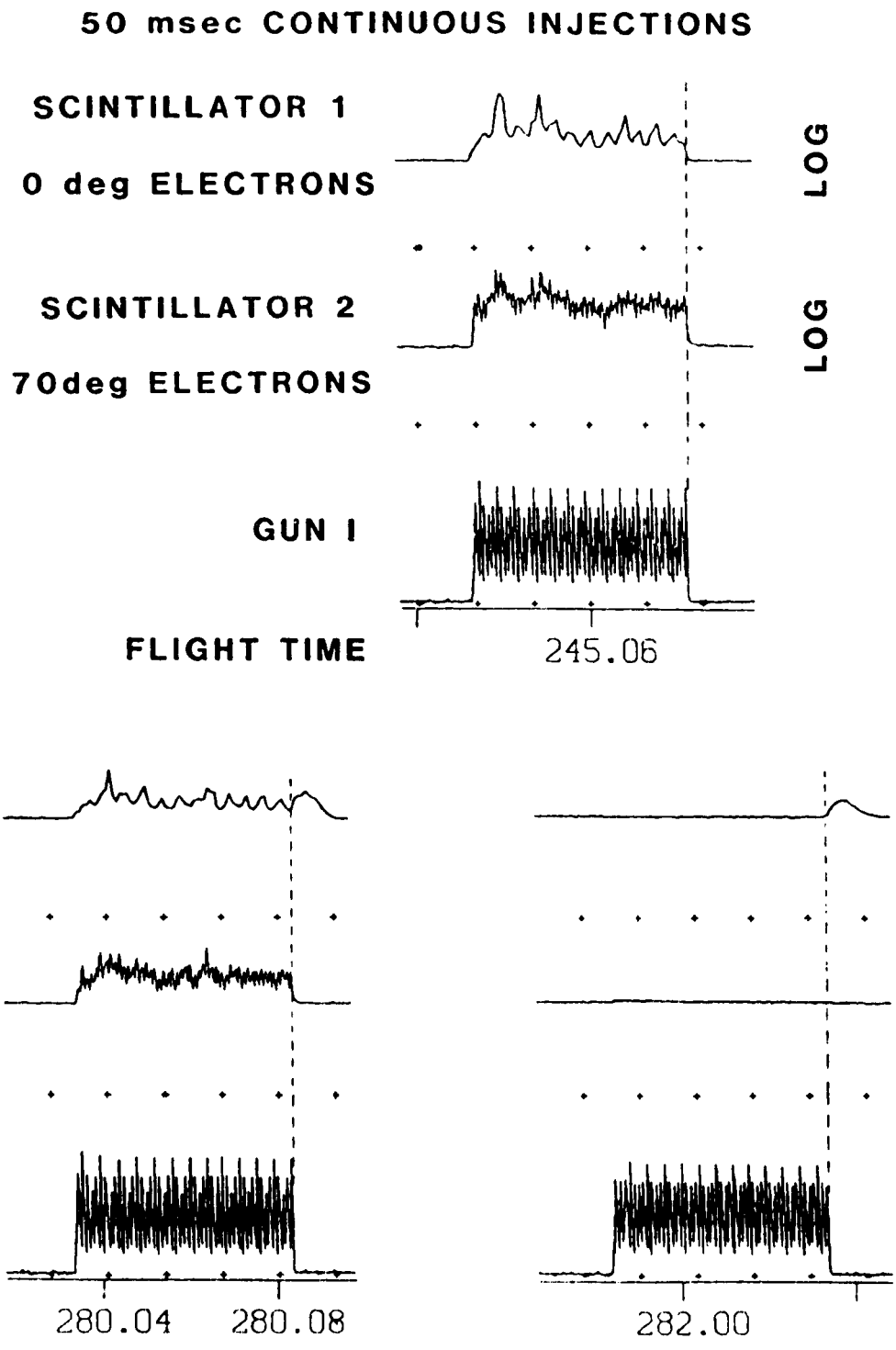
50 msec CONTINUOUS INJECTIONS
SCINTILLATOR 1
0 deg ELECTRONS
LOG
SCINTILLATOR 2
70deg ELECTRONS
LOG
GUN I
FLIGHT TIME
245.06
280.04
280.08
282.00
WITH ACS GAS

FIGURE 6

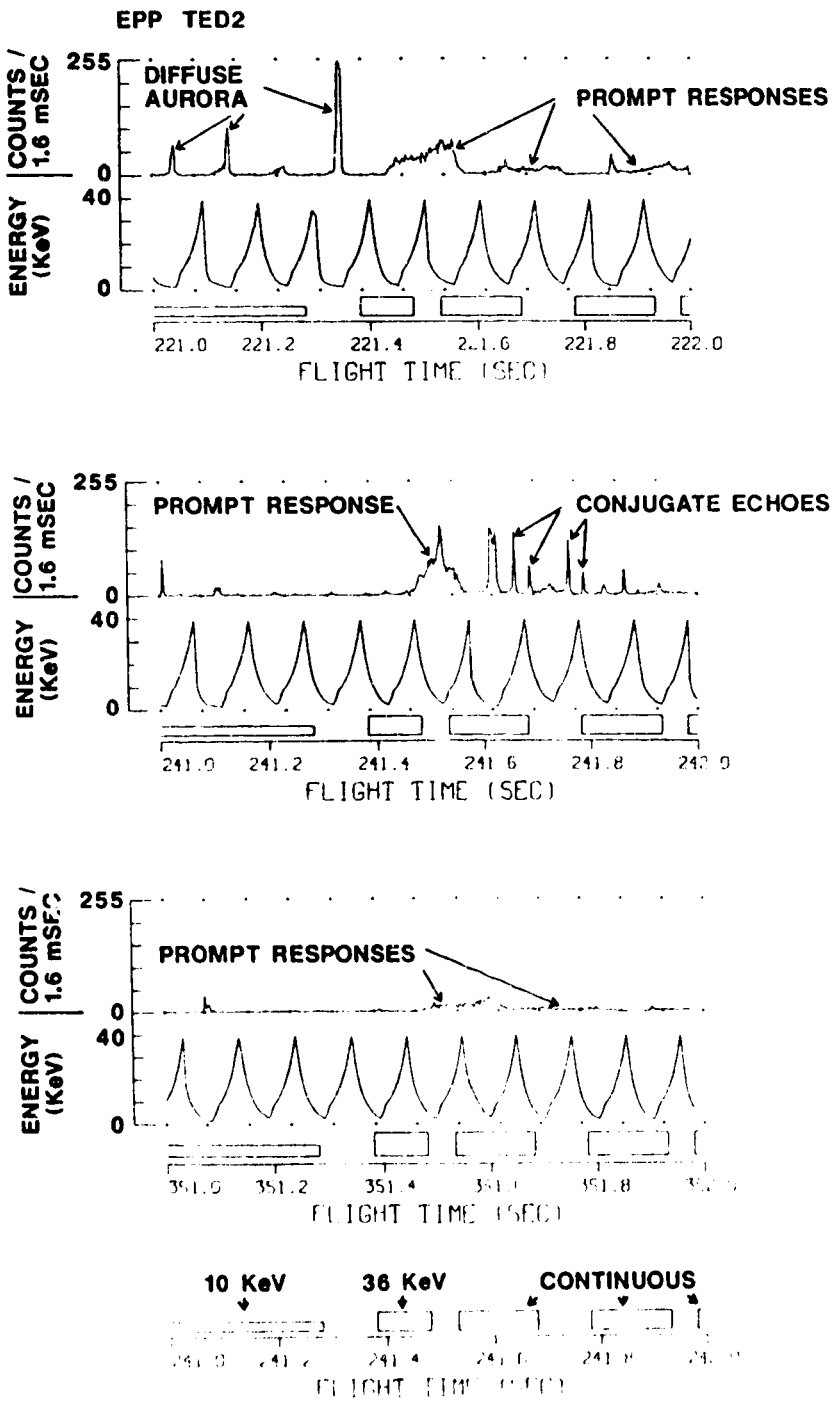
EPP TED2
COUNTS / 1.6 mSEC
255
0
DIFFUSE AURORA
PROMPT RESPONSES
ENERGY (KeV)
40
0
221.0
221.2
221.4
221.6
221.8
222.0
FLIGHT TIME (SEC)
COUNTS / 1.6 mSEC
255
0
PROMPT RESPONSE
CONJUGATE ECHOES
ENERGY (KeV)
40
0
241.0
241.2
241.4
241.6
241.8
FLIGHT TIME (SEC)
COUNTS / 1.6 mSEC
255
0
PROMPT RESPONSES
ENERGY (KeV)
40
0
351.2
FLIGHT TIME (SEC)
10 KeV
36 KeV
CONTINUOUS

FIGURE 7

PROMPT RESPONSE DELAY FOR OUT INJECTIONS

EPP TED2

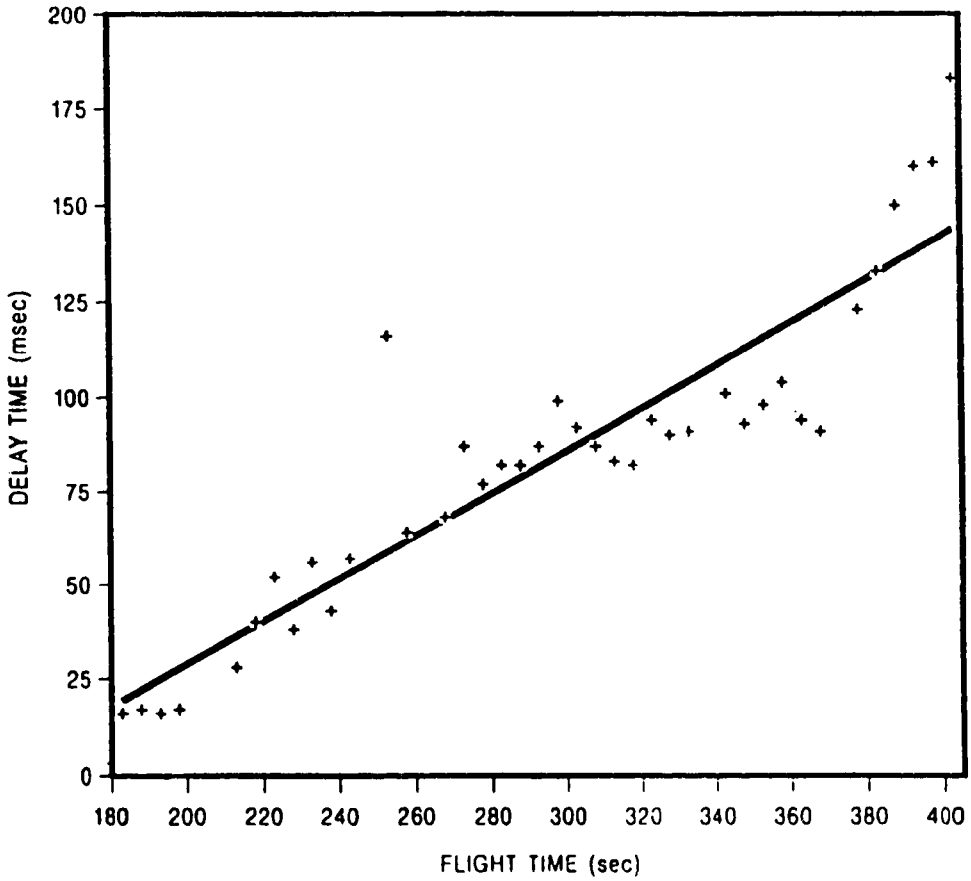

FIGURE 8

PROMPT RESPONSE AMPLITUDE FOR OUT INJECTIONS

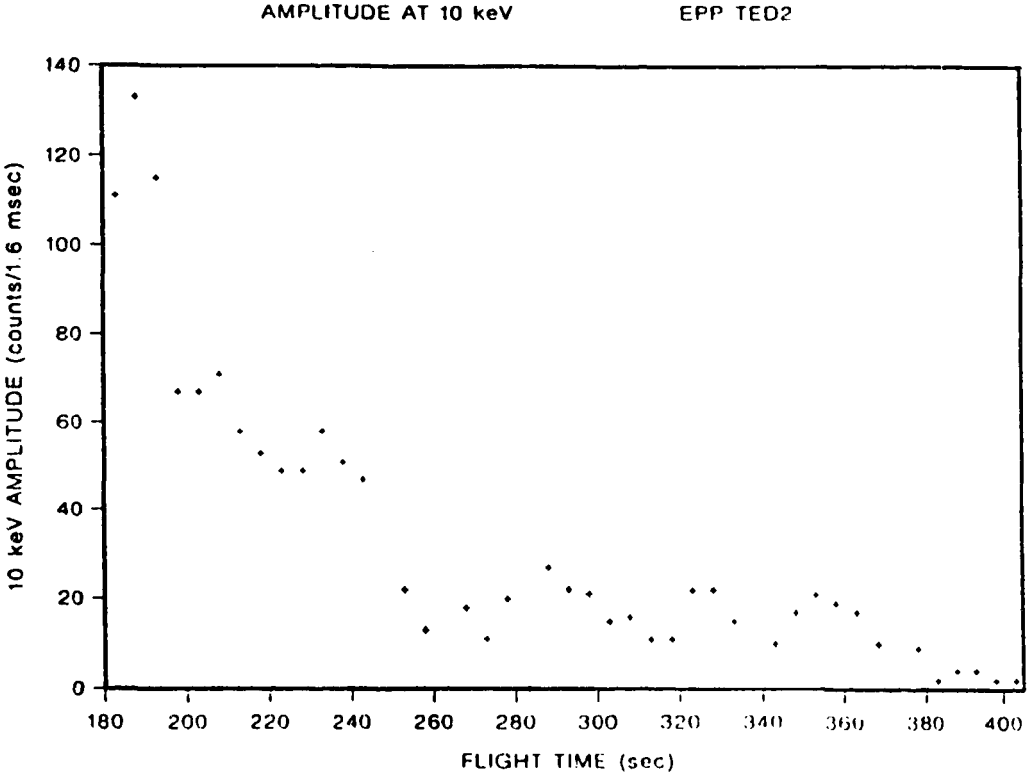

FIGURE 9

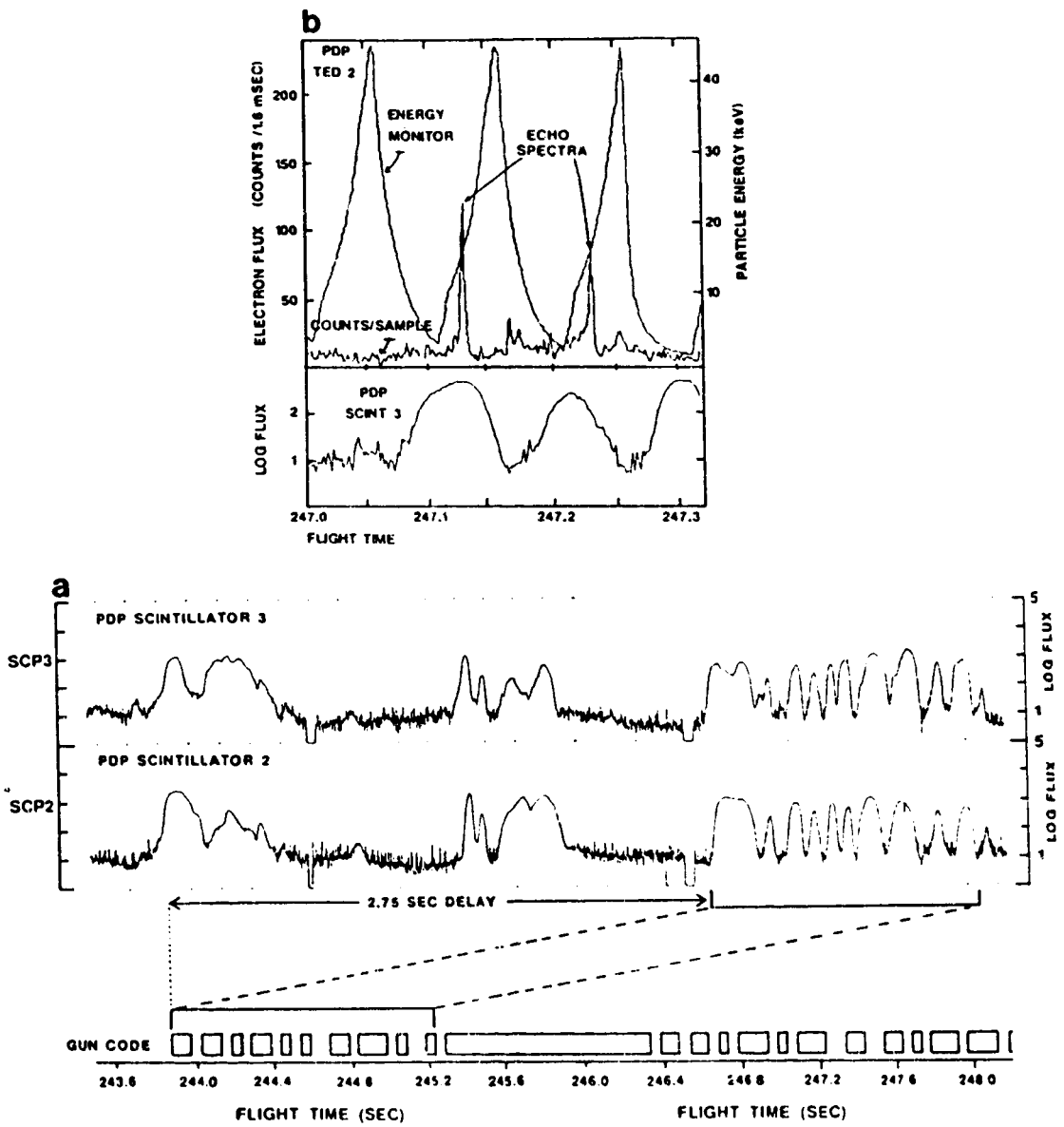
b
PDP
TED 2
ENERGY
MONITOR
ECHO
SPECTRA
ELECTRON FLUX (COUNTS /1.6 mSEC)
PARTICLE ENERGY (keV)
COUNTS/SAMPLE
PDP
SCINT 3
LOG FLUX
FLIGHT TIME
a
PDP SCINTILLATOR 3
SCP3
PDP SCINTILLATOR 2
SCP2
LOG FLUX
2.75 SEC DELAY
GUN CODE
FLIGHT TIME (SEC)
FLIGHT TIME (SEC)

FIGURE 10

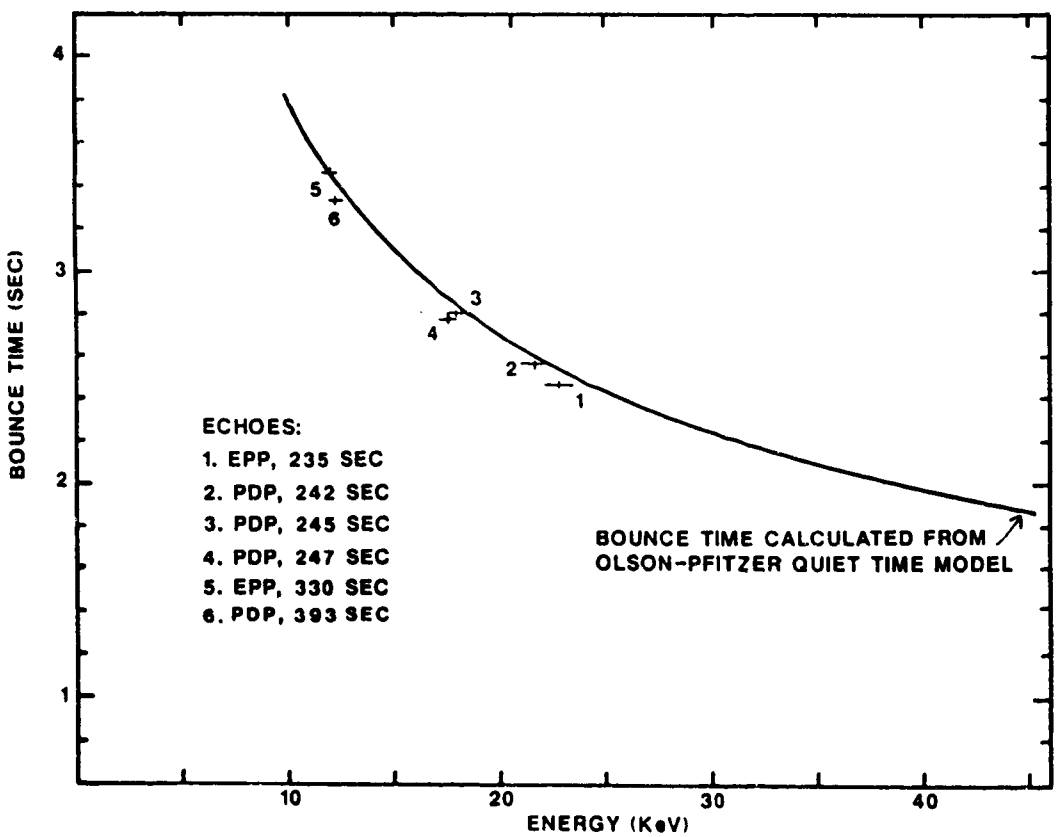
BOUNCE TIME (SEC)
4
3
2
1
10
20
30
40
ENERGY (KeV)
5
6
3
4
2
1
ECHOES:
1. EPP, 235 SEC
2. PDP, 242 SEC
3. PDP, 245 SEC
4. PDP, 247 SEC
5. EPP, 330 SEC
6. PDP, 393 SEC
BOUNCE TIME CALCULATED FROM
OLSON-PFITZER QUIET TIME MODEL

FIGURE 11